RSC Advances

PAPER

View Article Online
View Journal | View Issue

Cite this: *RSC Adv.*, 2018, **8**, 28746

Catalytic and anti-bacterial properties of biosynthesized silver nanoparticles using native inulin†

Wei Xu, *[ade] Kunling Huang,[a] Weiping Jin,[b] Denglin Luo,[c] Huan Liu,[a] Yingying Li[a] and Xinfang Liu[a]

Silver nanoparticles (Ag NPs) were green synthesized using native inulin as the reducing and capping agent with varied incubation temperatures, incubation times and Ag^+ concentrations. The biosynthesized Ag NPs were characterized using UV-visible spectroscopy, Field Emission Transmission Electron Microscopy (FE-TEM) and X-ray powder diffraction. The UV visible spectra of the Ag NPs revealed a characteristic surface plasmon resonance peak at 420 nm. FE-TEM showed that the biosynthesized Ag NPs were spherically shaped and monodispersed nanoparticles. The sizes were 18.5 ± 0.9 nm and 20.0 ± 1.2 nm for the Ag NPs synthesized at 80 °C and 100 °C for 2 h using 0.1% inulin and 2 mM Ag^+. Their PDIs were 0.180 ± 0.05 and 0.282 ± 0.13, respectively. Improving the incubation temperature, incubation time and silver nitrate concentration promoted Ag NP synthesis. The prepared Ag NPs were effective in the catalytic reduction of 4-NP and in inhibiting the growth of bacteria. The inhibition zone could reach 10.21 ± 2.12 mm and 9.92 ± 0.50 mm for *Escherichia coli* and *Staphylococcus aureus*. The kinetic rate constant (k_{app}) could reach 0.0113 s^{-1}, and the maximum inhibitory zones were 10.21 ± 2.12 mm and 9.92 ± 0.50 mm, respectively, for the two microorganisms. This biosynthesis illustrates that native inulin could be a potential candidate in the green fabrication of Ag NPs, and this is promising in catalytic and bacteriostatic fields.

Received 20th April 2018
Accepted 30th July 2018

DOI: 10.1039/c8ra03386b

rsc.li/rsc-advances

1. Introduction

Silver nanoparticles (Ag NPs), a type of noble metal nanoparticle, have emerged as promising antimicrobial agents, light-sensitive materials and sensing elements, and have been widely applied in the cosmetic, textile, medical and food industries.[1–4] Recently, biosynthesis has been suggested as a potential alternative for Ag NP fabrication. Simplicity, cost effectiveness, high compatibility and low toxicity are common advantages during Ag NP formation.[5–7] As a result, extensive interesting investigations have been conducted to green synthesize Ag NPs.

By masterly utilizing bioconversion, bacteria and fungi have been used for simple and eco-friendly synthesis methods.[8] Besides this, active substances or plant extracts have been verified as ways to effectively biosynthesize Ag NPs.[9,10] *Coffea arabica* seed extract,[11] leaf extracts,[12] tea extract[13] and polyphenols[14] have been backed to biosynthesize Ag NPs. Polysaccharides, a kind of native biomacromolecule, have shown promise for Ag NP biosynthesis. Starch,[15] guar gum and [16] cellulose[17] have been practiced to green synthesize Ag NPs. In our previous investigations, we have green synthetized Ag NPs using xanthan gum and found that the aggregation of Ag NPs was related to the xanthan gum conformation transition of denaturation and renaturation. The excellent antibacterial effect and catalytic capability of 4-nitrophenol reduction were further documented.[18] However, green synthesis of Ag NPs using native inulin has scarcely been reported.

Native inulin is a water soluble fructose-based polymer. As a dietary fiber from nature, inulin is a fructan varying in the degree of polymerization (DP) from 2 to 60. It is found in various grains, fruits and vegetables. Native inulin is usually extracted from chicory or Jerusalem artichokes.[19] It has been reported that inulin has many health benefits, including regulating blood glucose.[20] Due to the excellent water-holding capacity of the gel, it is commonly used as a modifier and functional ingredient in the food field.[21] In this paper, we explore the biosynthesis of Ag NPs using native inulin. The catalytic and antibacterial properties were further investigated. This endeavor provided a feasible method for Ag NP biosynthesis with excellent antibacterial and catalytic properties which may facilitate their use in medical, food, and biological applications.

[a]*College of Life Science, Xinyang Normal University, Xinyang, 464000, China. E-mail: toxuwei1986@163.com*

[b]*College of Food Science and Engineering, Wuhan Polytechnic University, Wuhan, 430023, China*

[c]*College of Food and Bioengineering, Henan University of Science and Technology, Luoyan, 471023, China*

[d]*Tea Plant Biology Key Laboratory of Henan Province, Xinyang, 464000, China*

[e]*Institute for Conservation and Utilization of Agro-bioresources in Dabie Mountains, Xinyang, 464000, China*

† Electronic supplementary information (ESI) available. See DOI: 10.1039/c8ra03386b

2. Materials and methods

2.1. Materials

Native inulin (DP 2-60) was obtained from the Cosucra Company (Belgium). Silver nitrate, 4-nitro-phenol (4-NP), sodium borohydride and other chemical reagents were purchased from commercial sources in China. Their solutions were prepared using ultrapure water from a Millipore (Millipore, Milford, MA, USA) Milli-Q water purification system.

2.2. Synthesis of the silver nanoparticles

For the synthesis of the silver nanoparticles, 0.1 mg of inulin was dissolved in 100 mL of ultrapure water under constant stirring (84-1A, Shanghai meiyingpu instrument Co. LTD) for 2 h to obtain a 0.1% (w/v) solution. Subsequently, $AgNO_3$ was added into the inulin solutions to get the final concentrations of 1 mM, 2 mM and 3 mM. The reaction mixtures were incubated for the time periods of 1 h, 2 h and 3 h at 80 °C and 100 °C under dark conditions with stirring.

2.3. Characterization

UV-visible spectroscopy (UV-vis) was performed using a UV/VIS/NIR Spectrometer (Lambda950, United States) as a function of temperature during the synthesis of the Ag NPs. The control was run as only 0.1% of the corresponding polysaccharide without a reducing agent. The hydrate particle size and zeta potential were measured using a commercial laser light scattering instrument (Zetasizer NanoZS, Malvern Instruments, United Kingdom) at 25 °C. Each sample was measured three times. A drop of the Ag NP colloidal solution was dispensed directly onto a carbon-coated copper grid and dried completely in a vacuum desiccator. Then the pictures of the prepared samples were obtained using a Field Emission Transmission Electron Microscope (FE-TEM) (G2 F20S, Hitachi, United States). The composition was also examined using energy-dispersive X-ray spectroscopy (EDX) with the FE-TEM. X-ray powder diffraction (XRD) was scanned over the range 2θ 5–85° using Cu Kα radiation with a scanning rate of 0.5° min^{-1}, 40 kV and 30 mA (Smartlab9, Japan).

2.4. Catalytic reduction of 4-NP

The catalytic 4-NP reduction was carried out in the same manner as in our previous reports.[22,23] Briefly, 10 mL of fresh $NaBH_4$ aqueous solution (0.2 M) was mixed with 10 μL of aqueous Ag NPs. Subsequently, 1 mL of 4-NP solution (2×10^{-3} M) was added into 1 mL of the above mixture. The

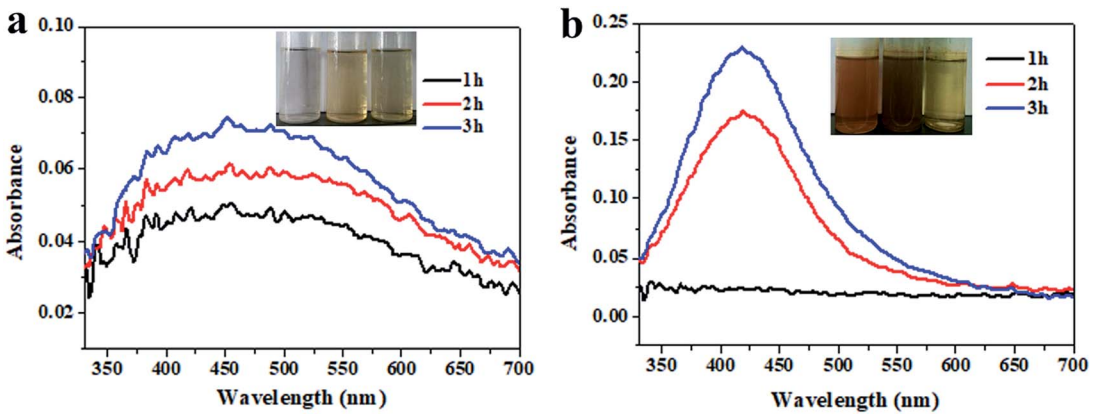

Fig. 1 UV-vis spectra of the Ag NPs as a function of reaction time incubated at 80 °C (a) and 100 °C (b) with 2 mM Ag^+ and 0.1% inulin.

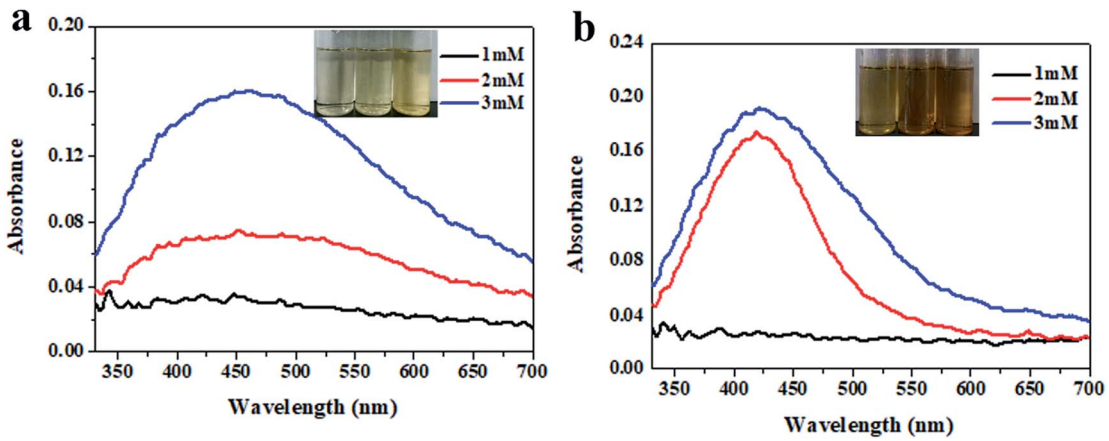

Fig. 2 UV-vis spectra of the Ag NPs as a function of Ag^+ concentration incubated at 80 °C (a) and 100 °C (b) for 2 h with 0.1% inulin.

concentrations of 4-NP and $NaBH_4$ in the reaction solution were finally 2×10^{-4} M and 0.1 M, respectively. The reaction was monitored by measuring the absorbance at 400 nm using a UV/VIS/NIR Spectrometer (Lambda950, United States).

2.5. Antibacterial assay

The green synthesized Ag NPs were tested for antimicrobial activity *via* the well diffusion method and modified dilution method against pathogenic bacteria, including Gram-negative *Escherichia coli* and Gram-positive *Staphylococcus aureus*. Briefly, filter paper discs (6 mm) were soaked in the formed Ag NP solution for 15 min, and then placed on the inoculated plates that cultured *Escherichia coli* and *Staphylococcus aureus*. The zones of inhibition were measured after incubation at 37 °C for 24 h. The dilution method was conducted by adding different volumes onto the inoculated plates that cultured *Escherichia coli* and *Staphylococcus aureus*. Then their growth after 24 h of incubation was observed.

3. Results and discussion

3.1. Effect of heating time on the Ag NP synthesis

In this study, native inulin was used as the reducing and stabilizing agent for the Ag NP synthesis. As shown in Fig. 1, the characteristic UV-vis spectra indicated that the Ag NPs had been green biosynthesized. The visual observation of the solution changing to a dark brownish yellow color further indicated the formation of Ag NPs, as this has been found in the results of other publications during Ag NP synthesis.[24] The absorption spectrum showed an intense band at around 420 nm that was

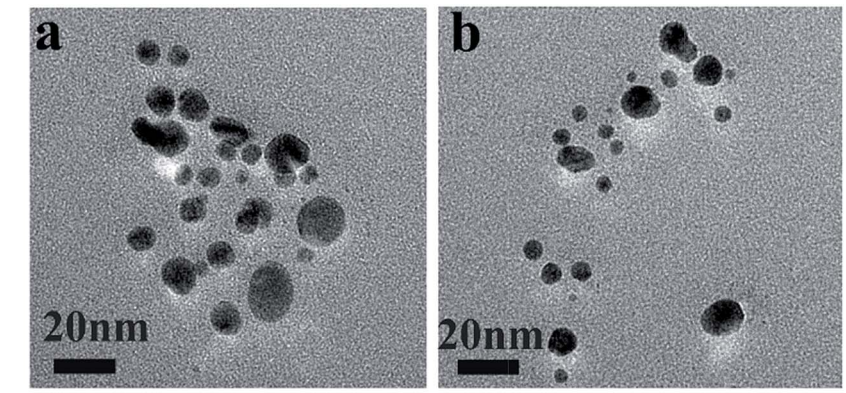

c

	Average Size (nm)	PDI	Zeta (mV)
Ag80 NPs	12.5±0.6	0.185±0.07	-0.95±0.12
Ag100 NPs	9.8±1.5	0.28±0.14	-0.18±0.05

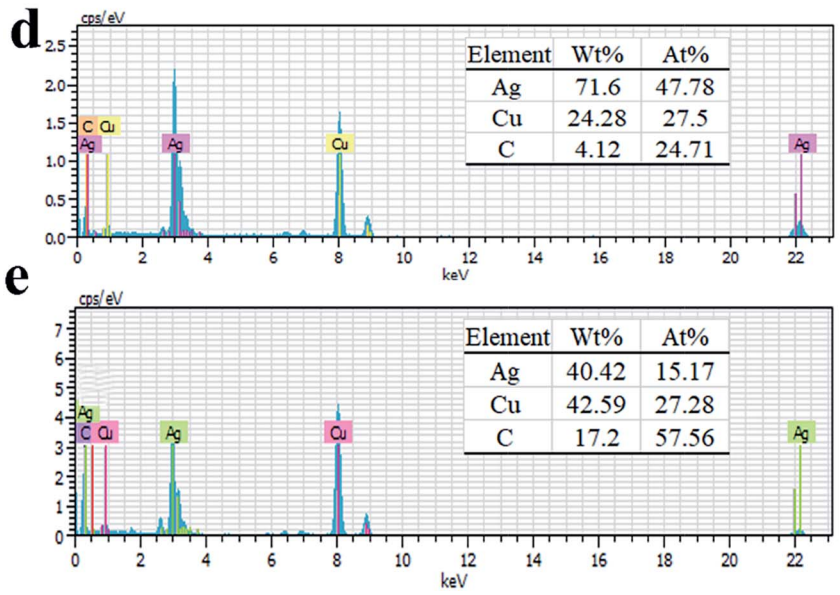

Fig. 3 FE-TEM images (a and b), size, PDI, zeta potential (c) and EDX (d and e) of Ag NPs synthesized at 80 °C (a and d) and 100 °C (b and e) for 2 h using 0.1% inulin and 2 mM Ag^+.

identified as a "surface Plasmon resonance band" and ascribed to the excitation of free electrons in the Ag NPs. Meanwhile, a higher incubation temperature promoted the reduction of the Ag NPs. The progressive absorption illustrated the gradual evolution of the Ag NP synthesis as the heating time increased. Inulin, classifying as either an oligo- or polysaccharide, belongs to the fructan carbohydrate subgroup. During the heating process, the increased number of hydroxyl groups on the inulin chain causes the active reduction of Ag^{+} to Ag^{0}.

3.2. Effect of Ag^{+} concentration on the Ag NP synthesis

The effect of the Ag^{+} concentration (1 mM, 2 mM and 3 mM) on the synthesis of the Ag NPs was investigated with 0.1% inulin after heating for 2 h at 80 °C and 100 °C (Fig. 2). Fig. 2 displays similar phenomena to Fig. 1. Obviously, the increasing brown colour change of the inset illustrates the easy synthesis of the Ag NPs with a higher Ag^{+} concentration. The increased absorption intensity with an increase in Ag^{+} concentration and a high incubation temperature simultaneously certify an enhanced reduction of Ag^{+}. It was noted that approximately 3 mM Ag^{+} needed to be provided at 80 °C incubation. Comparatively, the phenomenon of the surface Plasmon resonance band was obvious when the Ag^{+} concentration was 3 mM and incubation was at 100 °C. After formation, the Ag NPs get embedded and stabilized within the inulin matrix as with other polysaccharides.[25] It has been illustrated that Ag NPs can be fabricated using glucose as the reducing agent, and impregnated into cellulose, microcrystalline cellulose, carboxymethyl cellulose and chitosan.[26]

3.3. Morphology of the synthesized Ag NPs

The morphology of the various Ag NPs fabricated using inulin was further investigate using FE-TEM. The results (Fig. 3a) clearly demonstrate that the Ag NPs were biosynthesized and exhibited an inerratic spherical appearance. It was noted that the inulin-based Ag NPs displayed excellent dispensability (Fig. S1†). When the incubation temperature increased from 80 °C to 100 °C, much more Ag NPs were synthesized. More interestingly, the size of the Ag NPs nearly remained unchanged. The hydrate particle sizes were 12.5 ± 0.6 nm and 9.8 ± 1.5 nm for the Ag NPs synthesized at 80 °C and 100 °C, respectively, for 2 h using 0.1% inulin and 2 mM Ag^{+}. These results were in agreement with the particle size distribution analysis of the TEM image (Fig. S2†). The PDIs were 0.185 ± 0.07 and 0.28 ± 0.14, respectively. The low PDIs illustrate the excellent distribution of the fabricated Ag NPs. This phenomenon may relate to the structure of the inulin matrix. In the same way as when treated with a thermal process, the exposed external hydroxyl groups exert the reduction effect and further combine with the Ag NPs, endowing them with their high stability. The EDX spectra further confirms the fabrication of the Ag NPs based on native inulin (Fig. 3d and e).

3.4. XRD analysis of the inulin-based Ag NPs

As Fig. 4 shows, inulin was amorphous. This well coincided with previous studies.[27] Meanwhile, the inulin-based Ag NPs showed distinctive characteristic diffraction peaks at 38° and 44°. These

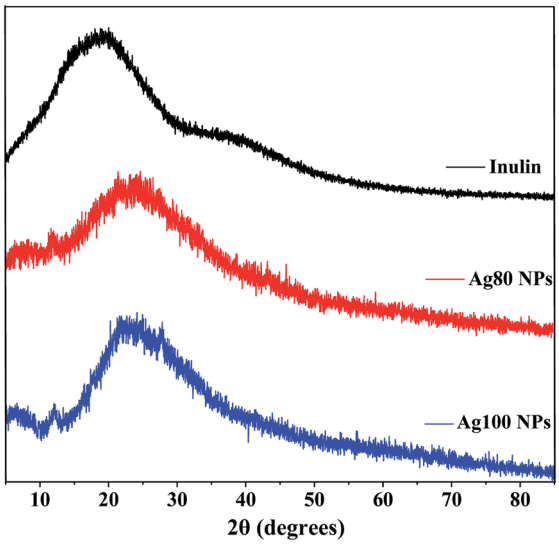

Fig. 4 XRD analysis of inulin and the Ag NPs synthesized at 80 °C and 100 °C for 2 h using 0.1% inulin and 2 mM Ag^{+}.

typical diffraction peaks possibly illustrate the formation of a face centered cubic structure. It was noted that the distinctive characteristic diffraction peaks were not intense enough. Additionally, strong peaks at 12.1° appeared during the inulin-based Ag NP synthesis. This may have been affected by the crystallization behavior of inulin during the freeze drying process. Furthermore, it was found that the diffuse peak of the inulin-based Ag NPs shifted as compared with that of inulin, which further confirmed the interaction between inulin and the Ag NPs during biosynthesis.

3.5. Catalytic behavior for the reduction of 4-NP

To compare the catalytic efficiency of the inulin-based Ag NPs, their catalytic behaviors were examined through the model reaction of 4-NP reduced by $NaBH_4$. Kinetic rate constant (k_{app}) values were calculated and were used to evaluate the catalytic behavior. The pseudo-first-order kinetics are often described as $\ln(C_t/C_0) = -k_{app}t$, where C_t is the concentration of 4-NP at time t, C_0 is the original concentration of 4-NP, and k_{app} is the degradation rate (Fig. 5). By comparing the k_{app} values of the green, synthetic Ag NPs at different conditions, it was easily found that k_{app} continuously increased as the incubation temperature increased and the time increased. When the incubation temperature was 80 °C and silver nitrate was at 2 mM, the k_{app} values were 0.0074 s^{-1}, 0.0086 s^{-1}, and 0.0093 s^{-1} when the incubation time was 1 h, 2 h and 3 h accordingly. In comparison, the value increased to 0.0085 s^{-1}, 0.0100 s^{-1} and 0.0113 s^{-1} for the Ag100 NPs, respectively. Even so, the k_{app} was noted to be more significantly affected by the concentration of silver nitrate. The k_{app} values of the Ag80 NPs were 0.0043 s^{-1} and 0.0113 s^{-1} when 1 mM and 2 mM Ag^{+} was provided. Meanwhile, the catalytic behavior clearly accelerated for the Ag100 NPs. The k_{app} accordingly increased to 0.007 s^{-1} and 0.0115 s^{-1}. This confirmed that all of the final conversion of 4-NP was below 4.5% (Fig. S3†). The high k_{app} was nearly equivalent to that of silver-

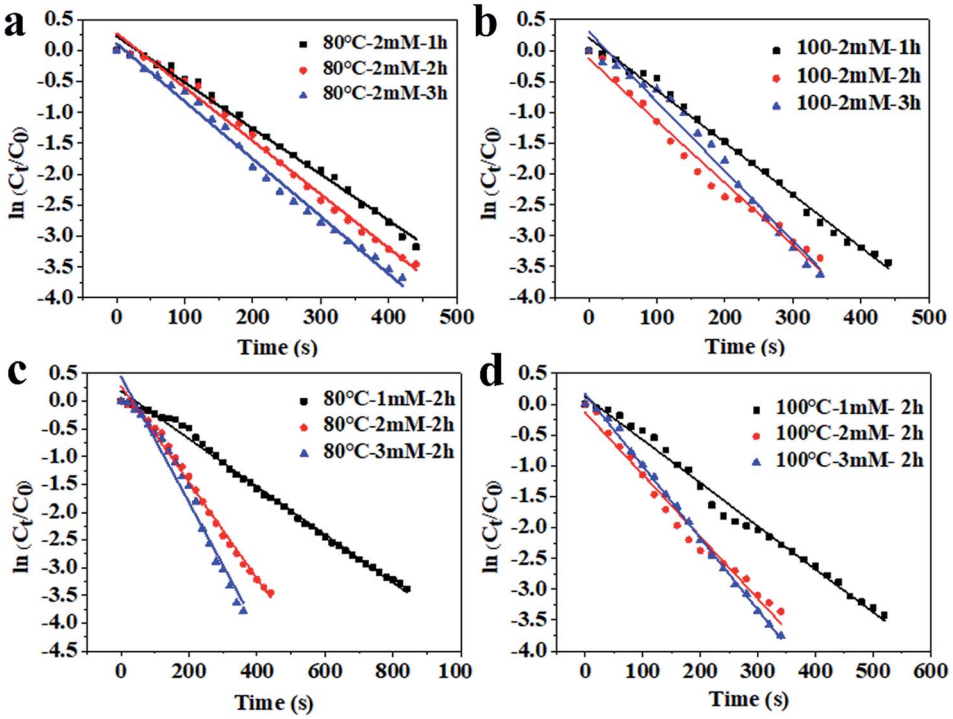

Fig. 5 The relationship between $\ln(C_t/C_0)$ and reaction time of the inulin-based Ag NPs synthesized at 80 °C (a and c) and 100 °C (b and d) with different Ag^+ concentrations.

deposited magnetic nanoparticles (1.5×10^{-2} s).[28] Compared with our published paper, the catalytic behavior equally matched that of the Ag NPs that were green biosynthesized using soluble green tea powder, in which the k_{app} values were 0.00918 s^{-1}, 0.00931 s^{-1} and 0.00941 s^{-1} when the reaction times were 20 min, 40 min and 60 min, respectively (Fig. 6).[29] As in the previous study, k_{app} mainly depended on the specific surface area and quantity of the Ag NPs.[30] This well coincided with the Ag NPs size and distribution shown in Fig. 1–3.

3.6. Antibacterial properties of the inulin-based Ag NPs

As Fig. 7 and Table 1 show, the antibacterial activity of the inulin-based Ag NPs was determined for the preparation conditions. The higher the incubation temperature and Ag^+ concentration, the higher the antimicrobial activity that was exhibited. When prepared at 80 °C with 2 mM Ag^+, the zones of inhibition for *Escherichia coli* and *Staphylococcus aureus* were 8.10 ± 0.20 mm and 8.11 ± 0.39 mm, respectively. Meanwhile for the Ag100 NPs, the inhibition zones increased to 9.93 ± 0.21 mm and 8.74 ± 0.36 mm. When 3 mM Ag^+ was used, the values further improved to 10.21 ± 2.12 mm and 9.92 ± 0.50 mm. This phenomenon may have resulted from the increasing concentration of Ag NPs as the incubation temperature and Ag^+ concentration increased. It was also noted that the antimicrobial activity was higher against *Escherichia coli* than it was against *Staphylococcus aureus*. This similar phenomenon was also backed by Jeeva. They found that the antibacterial activity of metallic silver nanoparticles synthesized using leaf extracts of

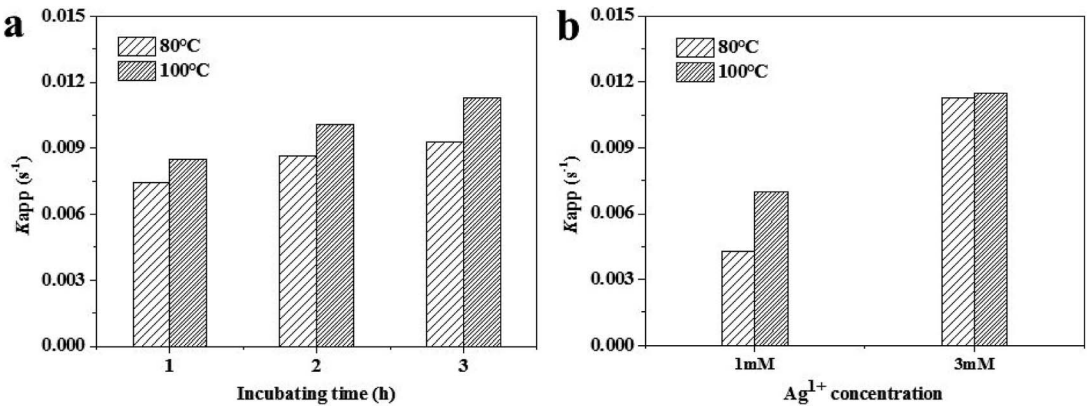

Fig. 6 Apparent rate constants, k_{app}, of the inulin-based Ag NPs synthesized at 80 °C and 100 °C with different Ag^+ concentrations.

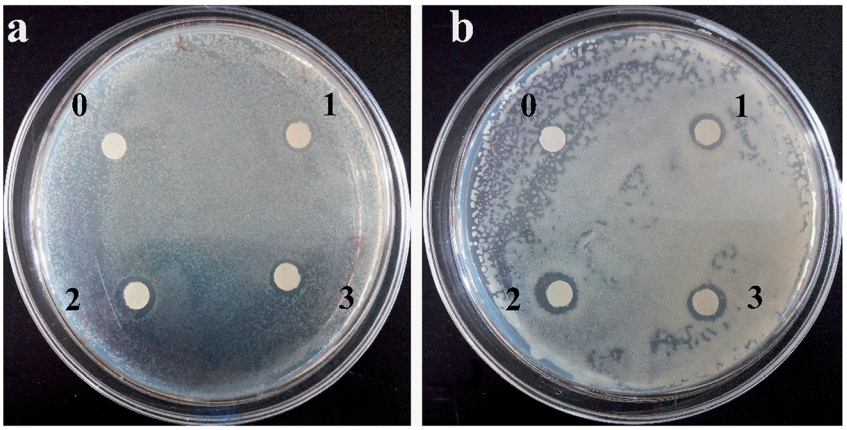

Fig. 7 Zone of inhibition of the inulin-based Ag NPs against *Escherichia coli* (a) and *Staphylococcus aureus* (b). 0: Inulin solution; 1: Ag NPs formed at 80 °C using 2 mM Ag^+; 2: Ag NPs formed at 100 °C using 2 mM Ag^+; 3: Ag NPs formed at 100 °C using 3 mM Ag^+. The reaction time was 2 h and inulin was at 0.1%.

Table 1 Zone of inhibition obtained *via* the disc diffusion method[a]

Components	*Escherichia coli* (mm)	*Staphylococcus aureus* (mm)
Inulin (0.1%)	NZ	NZ
Sample 1	8.10 ± 0.20c	8.11 ± 0.39c
Sample 2	9.93 ± 0.21b	8.74 ± 0.36c
Sample 3	10.21 ± 2.12a	9.92 ± 0.50b

[a] NZ represents no result through visual interpretation. The samples were the same as in Fig. 7. Different letters indicate significant differences ($p \leq 0.05$).

Caesalpinia coriaria displayed a much higher antimicrobial activity against *Escherichia coli*.[31] In comparison, for our published xanthan gum-based Ag NPs, the antibacterial activity related to the conformation of xanthan, and displayed relatively low bacteriostatic ability (*S. aureus* was about 12.3 mm, and it was 10.7 mm for *E. coli*). This also confirms that the antibacterial activities are determined by the employed polysaccharide.[18] The different antibacterial behaviors may be related to the adsorption to the cell membrane that is determined by the stabilizer. Fig. 8 further verified, through visual interpretation, the antibacterial behavior of inulin-based Ag NPs. The antibacterial capacities well agreed with Fig. 7 and Table 1. When the addition was 200 μL, the inhibition rates could reach 98 ± 3% for *Escherichia coli* when the Ag NPs were formed at 100 °C using 3 mM Ag^+. Meanwhile for *Staphylococcus aureus*, the inhibition rates were 88 ± 1.5%. These results well coincided with the results of Fig. 7. The antibacterial properties of the inulin-based Ag NPs may be caused by how efficiently the NPs get attached to the cell membrane and penetrate inside the bacteria. The permeability of the cell membrane was ultimately changed, or the Ag NPs interacted with protein or DNA, which further led to bacteria death.

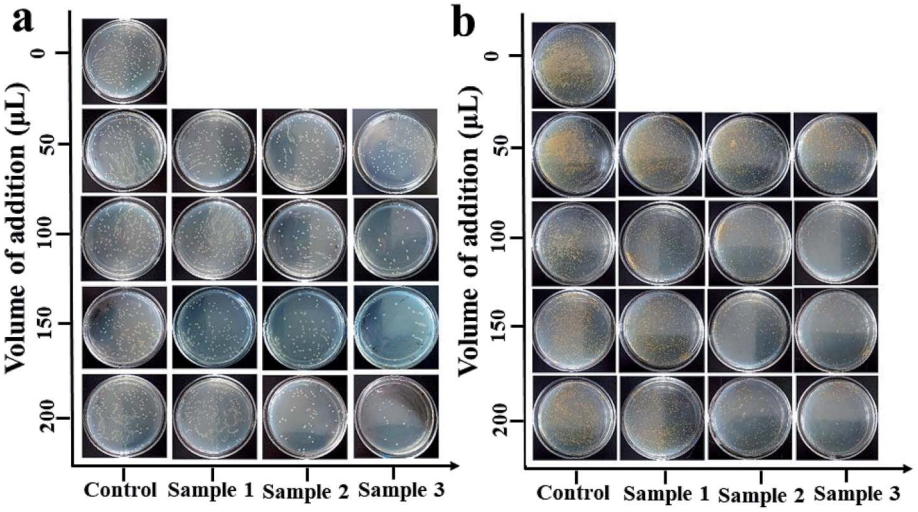

Fig. 8 Antibacterial behavior of inulin-based Ag NPs against *Escherichia coli* (a) and *Staphylococcus aureus* (b). Control: without addition; sample 1: Ag NPs formed at 80 °C using 2 mM Ag^+; sample 2: Ag NPs formed at 100 °C using 2 mM Ag^+; sample 3: Ag NPs formed at 100 °C using 3 mM Ag^+. The reaction time was 2 h and inulin was at 0.1%.

4. Conclusions

Water dispersible Ag NPs with excellent dispersion were bio-synthesized using inulin through a one spot thermal incubation. The synthesized Ag NPs exhibited an inerratic spherical appearance. When the incubation temperature was 80 °C and the Ag^+ concentration was 2 mM, the k_{app} values were 0.0074 s^{-1}, 0.0086 s^{-1} and 0.0093 s^{-1} when the incubation times were 1 h, 2 h and 3 h accordingly. In comparison, the values increased to 0.0085 s^{-1}, 0.0100 s^{-1} and 0.0113 s^{-1} for the Ag100 NPs, respectively. A bacteriostatic test illustrated that the fabricated Ag NPs had antimicrobial activity against *Escherichia coli* and *Staphylococcus aureus*. The maximum inhibitory zones reached 10.21 ± 2.12 mm and 9.92 ± 0.50 mm, respectively. These results verified that native inulin could be effective as a reducing agent and stabilizer for Ag NP fabrication. Their antibacterial and catalytic activities confirmed that inulin-based Ag NPs may be good candidates for use in biological and chemical fields.

Conflicts of interest

There are no conflicts to declare.

Acknowledgements

This work was financially supported by the National Natural Science Foundation of China (Grant No. 31701647), the Natural Science Foundation of Henan province (Grant No. 162300410229), and the Nanhu Scholars Program for Young Scholars of XYNU.

References

1 Z. M. Mahdieh, S. Shekarriz, F. A. Taromi and M. Montazer, *Cellulose*, 2018, **25**, 2355–2366.
2 S. K. Srikar, D. D. Giri, B. P. Dan, P. K. Mishra and S. N. Upadhyay, *Green Sustainable Chem.*, 2016, **6**, 34–56.
3 Y. Shao, C. Wu, T. Wu, S. Chen, T. Ding, X. Ye and Y. Hu, *Int. J. Biol. Macromol.*, 2018, **111**, 1281–1292.
4 I. Ghiuţă, D. Cristea, C. Croitoru, J. Kost, R. Wenkert, I. Vyrides, A. Anayiotose and D. Munteanu, *Appl. Surf. Sci.*, 2018, **438**, 66–73.
5 I. Rasaee, M. Ghannadnia and S. Baghshahi, *Microporous Mesoporous Mater.*, 2018, **264**, 240–247.
6 S. C. G. KirubaDaniel, L. AlbinaNirupa Julius and S. SivaGorthi, *Sens. Actuators, B*, 2017, **238**, 641–650.
7 T. Rasheed, M. Bilal, H. M. N. Iqbal and C. L. Li, *Colloids Surf., B*, 2017, **158**, 408–514.
8 I. Aiad, M. I. Marzouk, S. A. Shaker, N. E. Ebrahim, A. A. Abd-Elaal and S. M. Tawfik, *J. Mol. Liq.*, 2017, **243**, 572–583.
9 M. T. Moustafa, *Water Science*, 2017, **31**, 164–176.
10 A. Barapatre, K. R. Aadil and H. Jha, *Bioresour. Bioprocess.*, 2016, **3**, 8.
11 V. Dhand, L. Soumya, S. Bharadwaj, S. Chakra, D. Bhatt and B. Sreedhar, *Mater. Sci. Eng., C*, 2016, **58**, 36–43.
12 L. Wang, Y. Wu, J. Xie, S. Wu and Z. Wu, *Mater. Sci. Eng., C*, 2018, **86**, 1–8.
13 M. Sökmen, S. Y. Alomar, C. Albay and G. Serdar, *J. Alloys Compd.*, 2017, **725**, 190–198.
14 S. Ferraris, M. Miola, A. Cochis, B. Azzimonti, L. Rimondini, E. Prenesti and E. Vernè, *Appl. Surf. Sci.*, 2016, **396**, 461–470.
15 J. Jung, G. M. Raghavendra, D. Kim and J. Seo, *Int. J. Biol. Macromol.*, 2017, **107**, 2285–2290.
16 E. S. Abdel-Halim, M. H. El-Rafie and S. S. Al-Deyab, *Carbohydr. Polym.*, 2011, **85**, 692–697.
17 A. Salama, *Environmental Nanotechnology, Monitoring & Management*, 2017, **8**, 228–232.
18 W. Xu, W. Jin, L. Lin, C. Zhang, Z. Li, Y. Li, R. Song and B. Li, *Carbohydr. Polym.*, 2014, **101**, 961–967.
19 D. Luo, L. Yun, B. Xu, G. Ren, P. Li, L. Xuan, S. Han and J. Liu, *Food Chem.*, 2017, **229**, 35–43.
20 M. Shoaib, A. Shehzad, M. Omar, A. Rakha, H. Raza, H. R. Sharif, A. Shakeel, A. Ansari and S. Niazi, *Carbohydr. Polym.*, 2016, **147**, 444–454.
21 D. Meyer, S. Bayarri, A. Tárrega and E. Costell, *Food Hydrocolloids*, 2011, **25**, 1881–1890.
22 X. An, Y. Long and Y. Ni, *Carbohydr. Polym.*, 2017, **156**, 253–258.
23 J. Xu, T. Zhou, L. Jia, X. Shen, X. Li, H. Li, Z. Xu and J. Cao, *J. Nanopart. Res.*, 2017, **19**, 103.
24 R. M. El-Shishtawy, A. M. Asiri, N. A. M. Abdelwahed and M. M. Al-Otaibi, *Cellulose*, 2011, **18**, 75–82.
25 D. Guo, G. Liu, X. Li, X. Tang, J. Zhang, X. Zhu and S. Jiang, *J. Bionanosci.*, 2015, **9**, 325–329.
26 A. G. Hassabo, A. A. Nada, H. M. Ibrahim and N. Y. Abou-Zeid, *Carbohydr. Polym.*, 2015, **122**, 343–350.
27 P. Glibowski and S. Pikus, *Carbohydr. Polym.*, 2011, **83**, 635–639.
28 K. S. Shin, J. Y. Choi, S. P. Chan, H. J. Jang and K. Kim, *Catal. Lett.*, 2009, **133**, 1–7.
29 W. Xu, Y. P. Fan, X. F. Liu, D. L. Luo, H. Liu and N. N. Yang, *Mater. Res. Express*, 2018, **5**, 1–8.
30 Y. Chi, J. Tu, M. Wang, X. Li and Z. Zhao, *J. Colloid Interface Sci.*, 2014, **423**, 54–59.
31 K. Jeeva, M. Thiyagarajan, V. Elangovan, N. Geetha and P. Venkatachalam, *Ind. Crops Prod.*, 2014, **52**, 714–720.

